Ultrastructural Defects in Stereocilia and Tectorial Membrane in ageing mouse and human cochleae

Anwen Bullen[1], Andrew Forge[1], Anthony Wright[1], Guy P Richardson[2], Richard J Goodyear[2], and Ruth Taylor[1]

[1]UCL Ear Institute, University College London, WC1X 8EE, UK

[2]Sussex Neuroscience, School of Life Sciences, University of Sussex, Falmer, Brighton, BN1 9QG, UK

Running Head: Damaged Stereocilia and Tectorial Membrane in Aged Mice and Humans

Associate Editor: Lisa Nolan

Keywords

Hearing, Age Related Hearing Loss, Cochlea, Hair Cell, Tectorin

Grant Information:

BBSRC: BB/M00659X/1

Rosetrees Trust: A528 JS15/M58-F1

Corresponding Author: Dr Anwen Bullen

Abstract (250 words)

The ageing cochlea is subject to a number of pathological changes likely to play a role in the onset of age-related hearing loss (ARHL). Although ARHL has often been thought of as the result of the loss of hair cells, it is in fact a disorder with a complex aetiology, arising from changes to both the organ of Corti and its supporting structures. In this study, we examine two ageing pathologies that have not been studied in detail despite their apparent prevalence; the fusion, elongation and engulfment of cochlear inner hair cell stereocilia, and the changes that occur to the tectorial membrane, a structure overlying the organ of Corti that modulates its physical properties in response to sound. Our work demonstrates that similar pathological changes occur in these two structures in the ageing cochleae of both mice and humans, examines the ultrastructural changes that underlie stereocilial fusion, and identifies the lost tectorial membrane components that lead to changes in membrane structure. We place these changes into the context of the wider pathology of the ageing cochlea, and identify how they may be important in particular for understanding the more subtle hearing pathologies that precede auditory threshold loss in ARHL.

Significance Statement (100 words)

Understanding the aetiology of ARHL is vital to effective prevention and therapy. Potential therapeutic approaches often focus on correcting a single or narrow range of pathological changes (for example, degeneration of hair cells or afferent synapses) but do not address other cochlear pathologies. The significance of this work is the detailed description of additional pathological changes that have been poorly appreciated in the literature to date, but are likely to have significant effects on hearing in ageing. This work will help to inform a more rounded picture of the causes of ARHL, and encourage broader approaches to prevention and therapy.

Introduction

Loss of hair cells from the organ of Corti occurs progressively with age in humans (Wright, 1982; Wright et al., 1987), and is considered a major factor underlying age-related hearing loss (ARHL). Progressive age-related hair cell loss also occurs in the vestibular sensory epithelia of humans and is thought to underlie the balance dysfunction, dizziness and vertigo that affects older people (Rauch et al., 2001). Age-related loss of cochlear hair cells and progressive hearing impairment with features similar to those of human ARHL have been shown in a variety of animal species including mice, gerbils, rats, guinea pigs and rhesus monkeys. Typically, outer hair cells (OHCs) which form part of the cochlear active amplifier but do not themselves transmit sound impulses to the auditory nerve, suffer proportionally greater losses than inner hair cells (IHCs), which are responsible for the detection and transmission of sound stimuli to the brain. These patterns seem to be preserved across species (Coleman, 1976; Engle et al., 2013; Keithley and Feldman, 1982; Kusunoki et al., 2004; Tarnowski et al., 1991; Wright, 1984; Wright et al., 1987). ARHL is often considered to be characterised by increase in auditory thresholds initially to sounds of high frequency, and spreading progressively to include successively lower frequency hearing that corresponds to hair cell loss in a pattern, initiated and most extreme in the basal end of the cochlea and progressively encompassing more apical regions. However, a comprehensive study of age-related hearing loss of the UK population (Davis, 1995) showed that reduction in auditory thresholds at the lowest frquencies as well as high frequencies, and a similarly extensive study of hair cell losses with ageing in humans (Wright, 1982) revealed a corresponding progressive loss of hair cells from the cochlear apex as well as from the base (Legan et al., 2014; Wright, 1982). The age-related death of hair cells has been associated with mitochondrial dysfunction, free radical production and stimulation of apoptosis pathways (Yamasoba et al., 2007).

Correlated with hair cell loss is the retraction and loss of spiral ganglion afferent nerve fibres, which synapse with IHCs (Bao and Ohlemiller, 2010), but recently it has been recognised that loss of afferent synaptic connections to inner hair cells may progress in the absence of any obvious hair cell loss or injury and without causing any recordable increase (decrement) in auditory thresholds. Such “synaptopathy” is now considered to be an important early age-related pathology. Evidence of this phenomenon has been identified in both humans and animals (Gleich et al., 2016; Kujawa and Liberman, 2015; Parthasarathy and Kujawa, 2018; Sergeyenko et al., 2013; Wu et al., 2018) and the neuronal loss may be selective, affecting first fibres with low thresholds and high spontaneous rates of activity (Schmiedt et al., 1996). These losses have been suggested to correlate with some of the early and more subtle signs of ARHL that precede auditory threshold shifts such as difficulties with discriminating speech in noise (Parthasarathy and Kujawa, 2018).

Changes also occur during ageing to the structures that surround and support the function of the organ of Corti, particularly the stria vascularis. This pathology manifests as structural changes, including a thinning of the stria identified in both humans (Suzuki et al., 2006) and animals (Ichimiya et al., 2000). At the ultrastructural and molecular level, marginal cells of the stria vascularis show mitochondrial degradation (Thomopoulos et al., 1997), retraction of their interdigitating processes (Gratton et al., 1996) and a reduction in the expression of the sodium-potassium pump that is vital for maintaining the high positive ‘endocochlear potential’ in the cochlear fluid that bathes the apical surface of the organ of Corti and is vital for its function (Schmiedt, 1996). Age-related loss of cells of the spiral ligament that may impact cochlear homeostasis has also been noted (Hequembourg and Liberman, 2001).

Ageing is a multifactorial process, affecting various tissues and cells in different ways, so it is unsurprising that there are deleterious effects at a variety of sites in the inner ear which together may contribute to the recordable age-related functional deficits in hearing and balance. In this paper we present data from our ageing studies in mice and humans, showing effects of ageing at two crucial sites that have not been examined in detail

105 previously: stereocilia and the tectorial membrane. Defects to these structures are likely to
106 affect the precision of sound encoding within the organ of Corti, and are potential
107 candidates for the causes of ARHL that occur prior to loss of auditory thresholds.

108

109 **Methods and Materials**

110 **Animals**

111 Inner ear tissues were obtained from male CBA/Ca mice aged between 10 weeks and 32
112 months. A single sex of mice was used to enable fair comparison of all samples, as there are
113 known differences between sexes in the severity of age related hearing loss (Guimaraes et
114 al., 2004). With the exception of electron tomography, which was performed on only a small
115 number of representative samples, at least 6 animals at 6-8 months, 12 months, 17-19
116 months, 23-26 months and 30-32 months were examined, one ear from each animal
117 prepared by one of the processing procedures outlined below and the other for a different
118 one. All procedures involving the use of animals were approved by UCL Animal Ethics
119 committee and performed with authority of a project licence from the British Home Office.

120 Animals were sacrificed by carbon dioxide inhalation according to schedule 1 procedures.
121 Auditory bullae were isolated and the inner ear tissues fixed by direct perfusion. Fixative was
122 gently injected via an opening at the apex of the cochlea, through a rupture of the round
123 window and opening the oval window. For scanning and transmission electron microscopy
124 the fixative was 2.5% glutaraldehyde in 0.1M cacodylate buffer with 3 mM $CaCl_2$, and for
125 immunolabelling was 4% paraformaldehyde in phosphate buffered saline (PBS). The intact
126 cochleae were decalcified in 4% EDTA for 48 hours at 4°C. Both left and right ears were
127 used for examination, and this was selected randomly.

128

129 **Auditory brainstem responses (ABR)**

Male mice were anaesthetised using intraperitoneal ketamine (Vetalor™; Pfizer UK Limited, 0.01 ml/g of 10 mg/ml) and medetomidine (Domitor, Orion Corporation, Finland, 0.005 ml/g of 0.1 mg/ml) and placed in a soundproof booth (Industrial Acoustic Company Ltd). Body temperature of the animals was maintained using a homeothermic blanket maintained at 37°C. Subdermal needle electrodes (Rochester Electro-Medical) were inserted at the vertex (active), mastoid (reference) and with the ground needle electrode in the hind leg. Recordings were obtained using TDT system 3 equipment and software (Tucker-Davis Tech., Alachua FL). Click stimuli and tone pips at 8,12,24,32 and 40 kHz, were presented at 80 dB SPL and then in decrements of 10 dB, and from the responses recorded the auditory threshold was determined by the lowest sound pressure level at which the ABR waveform could be recognised. If no response was detected at the maximum stimulus level (80dB), a threshold of 90dB was recorded for subsequent graphical representation.

Statisitics

As ABRs were performed on the same groups of male mice as they aged (with animals sacrificed for cochleae analysis at each time point), ABR data was compared using a repeated measures ANOVA with Greenhouse-Geisser correction to account for violations of sphericity where required. Sphericity determined by Mauchly's test. P-value and corrected degress of freedom are reported. Calculations were carried out in SPSS (SPSS version 26, IBM, New York, USA, SCR_002865).

Transmission Electron Microscopy and Electron Tomography of mouse inner ears.

Fixed, decalcified cochleae were post-fixed and stained with osmium tetroxide and uranyl acetate, before dehydration through a graded series of ethanols and embedding in an Epon resin. Samples for electron tomography were incubated in a solution of 0.1% tannic acid in 0.1M cacodylate buffer before post-fixation and staining.

Sections of the entire intact inner ear were cut at several different depths through the cochlea and sections for examination were collected at each of these depths. Following initial examination by light microscopy of 1 µm thick sections stained with toluidine blue, for routine TEM, serial 100 nm thick sections were collected at each depth through the cochlea and placed on uncoated copper grids, stained with lead citrate and uranyl acetate and imaged at 80 kV in a JEOL JEM-1200 EX II transmission electron microscope. For electron tomography 200 nm sections on formvar-carbon coated copper grids were stained similarly and 10nm gold particles were applied as fiducial markers. Sections were imaged in a JEOL JEM-2100 microscope operating at 200 kV. Dual axis tomogram tilt series were collected at 1° increments for an axis of -60 to +60° and a pixel size of 0.371nm.

Electron Tomography Reconstruction

Reconstruction of electron tomography datasets was carried out using etomo, part of the IMOD programme suite (Kremer et al., 1996). Tomograms were reconstructed using weighted back projection with an applied SIRT-like filter equal to 5 iterations. Segmentation was carried out using the 3DMOD programme. For drawn objects contours were manually drawn or traced using assisted (livewire) segmentation at Z-axis intervals of 1.85 nm. Microtubules were modelled using point modelling with representative tubes. Isosurface rendering was carried out using the isosurface tool included in the IMOD package and were rendered across the complete Z-axis of the reconstructed images (excluding surface gold particles).

Scanning Electron Microscopy of mouse inner ears.

Organs of Corti and utricular maculae and cristae were dissected from the fixed, decalcified inner ears, post-fixed in OsO_4 and processed through the thiocarobohydrazide-Os-repeated procedure (Davies and Forge, 1987) before dehydration in an ethanol series, critical point drying and sputter coating with platinum. Samples were examined in a JEOL 6700F SEM operating at 5kV by secondary electron detection.

Scanning Electron Microscopy of Resin Sections

Samples were prepared as for transmission electron microscopy. Sections of 100 nm thickness were collected on Kapton tape in an automatic tape ultramicrotome (ATUM) (RMC, USA) as described previously (Bullen, 2019). Sections on tape were mounted on conductive carbon tape on silicon discs, coated with 12 nm of carbon and examined in a JEOL 6700F SEM operating at 5kV by backscattered electron detection. Image montages (~100 images) were automatically collected, stitched and normalised by SEM Supporter software (System In Frontier, Japan).

Immunohistochemical labelling of frozen sections of mouse ears

Paraformaldehyde fixed, decalcified intact cochleae were incubated overnight at 4°C in 30% sucrose solution, embedded in low-temperature-setting agarose (Sigma), oriented and mounted on specimen support stubs using OCT and then frozen. Frozen sections were cut at 15 µm and collected on polylysine coated slides (Polysine™, VWR). Tissue was permeabilised in 0.5%Triton in PBS for 20 minutes and the sections then incubated in blocking solution (10% goat serum in PBS with 0.15% Triton X-100). Tissue was incubated in primary antibody overnight at 4°C rinsed thoroughly in several changes of PBS and then incubated with appropriate secondary antibody conjugated to a fluorophore for 90 minutes at room temperature. A fluorescent phalloidin conjugate was added at 1µg/ml to the secondary antibody solution. Samples were mounted on to slides using Vectashield with DAPI (Vector Laboratories) to label nuclei and examined and imaged on a Zeiss AxioImager widefield microscope. The primary antibodies used were a rabbit polyclonal to mouse α-tectorin (TECTA) (Legan et al., 2014), a rabbit polyclonal to chick β-tectorin (TECTB) (R7, (Knipper et al., 2001) and a rabbit polyclonal to mouse carcinoma and embryonic antigen-related cell adhesion molecule 16 (CEACAM16) (Zheng et al., 2011).

Human tissue: Scanning electron microscopy of organ of Corti

From an archive of samples prepared for *electron microscopy* during the 1980's, organs of Corti from individuals with no known auditory pathology prior to death were *re*-examined. The archive contained 30 samples; 22 male and 8 female; mean age 56.8; age range 17-81. Female samples: mean age 55.3, age range 26-76. Male samples: mean age 56.5, age range 17-81. Procedures were performed in accordance with the UK legislation in force at the time; in the UK in the 1980's, the standard hospital post-mortem form allowed for removal of tissues other than for the purposes of transplantation provided the relatives' consent had been obtained. Appropriate consent was obtained for all samples used in this study. Within 40 minutes of death a tympano-meatal flap was raised and the stapes removed. An angulated blunt needle was used to perforate the round window membrane and 5 ml of 2.5% glutaraldehyde/2% formaldehyde in 0.1 M sodium cacodylate buffer with 2 mM calcium chloride at pH 7.25 was gently perfused through the cochlea. The two windows were sealed with Plasticine. A small cube of the temporal bone containing the labyrinth was then removed and placed in fresh fixative. The delay between death and removal of the labyrinth was never more than eighteen hours. The bones were then re-perfused with the glutaraldehyde/formaldehyde fixative and left for twenty-four hours before re-perfusion with buffer then perfusion with 1% OsO_4. The two windows were again sealed and the specimen was left for two hours. The osmium was washed out with buffer then 50% ethanol and the specimen was dissected under 50% alcohol to reveal the membranous labyrinth. The stria vascularis was removed as was the tectorial membrane. The spiral lamina was dissected in segments from apex to base; photographed then stored in 70% ethanol. The specimens were dehydrated in an ethanol series before critical point drying from liquid CO_2. The specimens were mounted on stubs using Araldite glue and then sputter coated with gold and palladium. Re-examination was of images taken after the original processing of the samples, or re-examination of samples as required. Re-examination of the samples was carried out on a JEOL 6700F SEM, operating at 5kV and using secondary electron detection. The samples did not show significant degradation when compared to archive images.

Human Temporal Bone Sections

Haematoxylin-eosin stained serial sections were taken from the archive of human temporal bone sections at the UCL Ear Institute. Accompanying medical notes were used to identify samples from patients whose recorded auditory deficits were ascribed to “presbycusis”. 3 male subjects with a presbycusis diagnosis were selected and examined along with 3 age and sex matched controls with no reported hearing deficit.

Results

Stereocilial fusion, elongation and internalisation are common features of ageing in both the mouse and human inner ear

CBA/Ca mice, unlike some other mouse strains, do not exhibit an accelerated loss of hearing with age. Fig. 1a shows auditory brainstem response (ABR) as a measure of hearing in a cohort of ageing CBA/Ca mice. The mice show loss of threshold with increasing age, particularly evident at the low frequency (apical) and the high frequency (basal) ends of the cochlea. The organs of Corti of 6-8 month old mice appeared normal: there was no obvious hair cell loss and hair bundles on both inner and outer hair cells (IHC, OHC) appeared intact (Fig. 1b-c). At approximately 12 months of age, there was no significant loss of OHC. The hair bundles of IHC scattered along the organ of Corti showed fusion of stereocilia (Fig. 1d). OHC hair bundles did not show fusion defects. At 18 and 24 months and later, although there was no obvious significant loss of IHC, even at 30 months of age, fused stereocilia persisted and became more prevalent (Fig. 1e-l). Fusions involved a variable number of stereocilia from doublets to an encompassing of almost the entire stereociliary bundle and appeared to be initiated in the longest row (Fig. 1j,l). Stereocilia were also often significantly elongated above the height of the longest stereocilia of the apparently unaffected hair bundles on adjacent IHC (Fig. 1k). Such “giant” stereocilia became more numerous and more elongated with age. Quantification of samples where a large region of the organ of

Corti was available at appropriate angles showed that at 6 months there were no fused or giant stereocilia observed, and no inner hair cell loss (n= 4 mice). By 12 months 8% of total IHC had evidence of stereocilial fusion, but no giant stereocilia were observed (n= 3 mice). By 24 months 20% of total IHC showed stereocilial fusion, and of these fusions 30% contained giant stereocilia. Giant stereocilia were only present on cells that also showed evidence of fusion. Giant stereocilia were also twice as common at the apical end of the cochlea as they were at the base (n= 5 mice). These observations indicate that following fusion of their stereocilia, IHC survive intact and the fused stereocilia continue to elongate. With increased age, there was increasing loss of OHC, but fusion of OHC stereocilia like that observed in IHC was not seen, suggesting that at least in OHC, stereociliary fusion is not an indicator of hair cell degeneration and incipient death.

Samples of the human organ of Corti from a 26 year old individual showed intact, normal appearing hair bundles on IHC and OHC across the cochlea (Fig. 2a-c). However in organs of Corti from elderly individuals (aged between 60-70), in addition to the expected loss of hair cells, fused and elongated stereocilia and evidence of their internalisation was apparent on some scattered IHC. Stereocilia become internalised into the apical cytoplasm, apparently through fusion of the stereociliary membrane with the apical plasma membrane (Fig. 2d-h insets and red arrows). Unlike in the mouse, giant, fused stereocilia were very occasionally evident on OHC (Fig. 2g). A comparison between mouse and human IHC shows the similar patterns of stereocilial fusion observed between the two species (Fig. 2h-i).

As we have previously reported (Taylor et al., 2015), fusion and elongation of stereocilia with ageing is also a feature of hair cells in vestibular sensory epithelia. In mice fusion of stereocilia in the absence of any obvious hair-cell loss was evident in utricular maculae and cristae by 12 -18 months (Fig. 3a). By 24 months, loss of hair cells was evident by their reduced density and patches where hair cells were entirely absent, whilst on remaining hair cells there was significant elongation of fused stereocilia (Fig. 3b,c). The fusion involved not

only the stereocilia but the kinocilium also became incorporated into the fused hair bundle. Similar fusion and elongation of stereocilia incorporating the kinocilium was also observed in the utricular maculae and cristae of elderly people (Fig. 3d,e) (Taylor et al., 2015). The presence of 'giant' fused stereocilia in IHC of the organ of Corti and hair cells of vestibular organs indicates that the addition of actin monomers to the stereocilia continues even after they are fused.

Internalisation of the stereocilia was more clearly defined in sections of IHC prepared for TEM, where seemingly intact stereociliary actin-filament bundles were enclosed beneath the apical plasma membrane, displacing the cuticular plate which became detached from the membrane (Fig. 4). Thin sections also showed that the cell bodies of IHC with fused, and internalised and/or giant stereocilia were intact with no obvious other signs of damage or degeneration (Fig. 4a,b,d,e), and that afferent terminals synapsing with these cells were mostly intact and not swollen (Fig. 4a,d). However, there were vesicles present in the region of the fusion, these vesicles appeared to be double membraned, and in some cases to have vesicular contents suggesting they may represent autophagic vesicles (Fig. 4d-e).

Actin bundles do not fuse after stereocilial fusion

Stereocilial fusion could have several potential effects on stereocilia structure, from fusion of only the stereocilial membranes to a breakdown of the organisation of the actin bundles. TEM sections through fused stereocilia appear to show that the actin bundles of the stereocilia remain intact despite the fusion (Fig. 4a,b). The densely packed actin filaments that normally form the rootlet are present, although they appear to be incorporated higher up the shaft of the stereocilium than we would normally expect, perhaps evidence of continued but dysregulated growth of the stereocilia. This is consistent with the observation from SEM data that fused bundles continue to elongate, indicating that actin structures are being maintained by the cell, although their growth may have become dysregulated. The plasma

membranes of the stereocilia do appear to fuse. Examination of fused stereocilia from a 1-year old mouse IHC by electron tomography shows similarly that the actin structures (visualised by isosurface rendering across a 200 nm section of stereocilia) do not appear to be disrupted by the fusion (Fig. 4f-g). Stereocilial rootlets are still clearly visible and well formed, and dividing lines between the actin bundles of different stereocilia are still visible, suggesting the bundles themselves have remained separated, and appear similar to neighbouring unfused stereocilia (Fig. 4f,g,h(ii),(iv),i(i)). However there is clear fusion between the membranes of several stereocilia (Fig. 4f,h(i)). In addition, tomographic reconstruction suggests that other cyto-skeletal components are also present in the fusion. Unfused IHC stereocilia are rooted into the cuticular plate, and little space exists in between the cuticular plate and cell membrane. However in both the tomogram and TEM sections, a space has developed between the cuticular plate and cell membrane in the region of the fusion (Fig. 4a,b,f-j). This space is occupied by microtubule like elements (red tubes) (Fig. 4g,j) as well as membranous structures (membrane cisterns) that could be divided into several different types; those without visible contents which were either greater than 100 nm in diameter (purple) (Fig4 g,j) or less than 100 nm in diameter (blue), those with cytoplasmic contents (orange), and tubular cisternae (white) (Fig. 4f, h(iii)) (supplementary movie S1). The microtubule elements appear to be reaching into the body of the stereocilial fusion (Fig. 4j(ii)).

The tectorial membrane undergoes significant structural changes with ageing

As well as fusion of IHC stereocilia, a remarkably consistent feature of the ageing mouse cochleae was a progressive degeneration of the tectorial membrane (TM). The normal characteristic appearance of the TM as described in detail elsewhere (Goodyear and Richardson, 2002; Goodyear and Richardson, 2018; Hasko and Richardson, 1988) was evident throughout the length of the cochleae in 6-8 month old mice. In sections for light microscopy stained with toluidine blue, the TM was characteristically shaped, overlying the

organ of Corti and attached to the spiral limbus on its medial side, and evenly stained (Fig. 5a). The sections showed a core composed of parallel, radially oriented quite closely packed collagen fibrils embedded within a uniform matrix, with denser regions on the upper surface, at the tip and on the lower surface, particularly in the ridge comprising the Hensen's stripe (Goodyear and Richardson, 2002). Subsequently, there was progressive degeneration of the TM that was first apparent in the apical coil from about 12-18 months then proceeded with age into the basal coil by 24-30 months (Fig. 5b-c). There was a decrease in the density of toluidine blue staining of the core of the TM, and changes in shape, initially a swelling and then often a thinning. As degeneration of the TM proceeded into the basal coil, it often became detached from the spiral limbus and the detached membrane came to lie against Reissner's membrane, this detachment also proceeded in an apex to base direction (Fig. 5c). The degeneration observed did not appear to be due to fixation artefacts in the tectorial membrane. All TMs examined from 6-8 month mice had the same appearance as that shown here (including many 6-8 month mice we have examined in the past that were not included in this study). The degeneration of the TM was also remarkably consistent in all ageing samples, including ageing mice we have examined for other studies. In addition, no other significant fixation artefacts were apparent in the organ of Cortis of the mice examined. This consistency and lack of associated fixation artefacts strongly suggests these effects are not due to fixation.

Changes in tectorial membrane are present in the cochleae of some humans with presbycusis

The tectorial membrane of an individual (55 years) with no known hearing deficit (Fig. 5d). showed similar structure to that of young mice. However, abnormalities of the TM were observed in sections of the temporal bones from two out of three individuals whose clinical notes attributed a hearing loss to "presbycusis". In one from an 81 year old male, the TM was remarkably thinner than normal (Fig. 5e). In the apical coil it was detached from the spiral limbus and attached to Reissner's membrane. In the middle coil it was displaced

towards Reissner's membrane but not attached to it (Fig. 5e). In a specimen from a 71 year old male, in the apical coil the TM was thinned and attached to Reissner's membrane, while in the basal coil it was distorted in shape but seemingly not attached to Reissner's membrane, although extracellular material exists between the two (Fig. 5f).

Loss of matrix components in aged tectorial membrane

TEM and electron tomography reconstructions revealed there was loss of the matrix components from the core of the TM (Fig. 6), but loss of collagen fibrils was also evident. The initial progression of degeneration of TM proceeded prior to any hair cell loss. Both IHC and OHC were present and apparently intact in the organ of Corti beneath degenerating TM. Degenerating TM was also evident in regions where there was no obvious significant loss of spiral ganglion neurons (Fig. 6a-b). The TM often appeared to become "motheaten"- with not only loss of matrix from the core but also apparent discontinuities in the collagen fibrillary structure. In some of the oldest animals examined, 24 -30 months, the core of the TM was almost entirely lost with only the initially dense fibrillary complexes on the upper and lower surface and at the tip remaining (Fig. 6c-f). electron tomography was carried out on a younger (1 year) specimen to ensure there would still be matrix material available to examine. Isosurface reconstruction showed that even by 1 year, the matrix material has begun to thin, leaving gaps in the membrane structure (Fig. 6g-h). This was evidenced by an overall reduction of the proportion of the reconstruction volume containing tectorial membrane components from 35% to 30%.

Degeneration of tectorial membrane is associated with loss of tectorins.

The major non-collagenous components of the TM are the glycoproteins TECTA, TECTB CEACAM16 and otogelin (Goodyear and Richardson, 2002) (Zheng et al., 2011). To establish whether the loss of protein constituents of the tectorial membrane was the cause of the structural degeneration observed, immunohistochemistry for TECTA, TECTB and CEACAM16 was performed. In the cochleae of mice at 6-8 months, antibodies to TECTA

(not shown) and TECTB labelled the TM equally intensely in all turns. The apical turn, which was the first to show degradation in older mice, is shown in Fig. 7a. At 18-19 months, the TM in the apical coil showed reduced labelling intensity in the core, but labelling still outlined the periphery and the labelling intensity in lower turns was greater and similar to that in the 6 month old mice for both TECTA and TECTB (Fig. 7b,c). Progressively with age, reduction in labelling intensity of the TM proceeded into lower coils and to the basal coil by 24-30 months (Fig. 7b,c). The loss of both TECTA and TECTB showed the same pattern of central to periphery loss and the base to apex gradient as seen in the cochleae of mice by light and electron imaging. The third matrix component CEACAM16, necessary for the formation of the striated sheet, showed a similar pattern of loss (Fig. 7d). Therefore, the loss of tectorial membrane density observed is likely due at least in part to the loss of these proteins from the TM representing a failure to maintain the matrix in older animals.

Discussion

Understanding the multi-factorial nature of ARHL is important to any form of effective treatment for presbycusis. Although traditionally hearing loss has been measured in terms of the loss of pure tone thresholds alone, more recently it has become clear that a variety of other changes to hearing occur before measurable threshold loss (Barbee et al., 2018). These deficits, known colloquially as “hidden hearing loss”, have been attributed largely to synaptopathies affecting a sub-population of the afferent nerves contacting IHC (Kujawa and Liberman, 2015). However, other changes to cochlear structure may also play a role. Stereocilia and the TM are both intimately involved in the mechanical to electrical transduction performed by cochlear hair cells. This study shows that fusion, elongation and internalisation of stereocilia on IHC, as well as degeneration and ultimately detachment of the TM from the spiral limbus are consistent features of ageing in the inner ear in mice and that identical or similar phenomena occur with ageing in humans. These changes can occur without significant loss of OHCs or IHCs. Consequently, the fusions and elongation of IHC

stereocilia and the degeneration of the TM have the potential to be contributors to early age-related decrements in hearing sensitivity.

Stereociliary abnormalities in IHCs

Fusion of stereocilia is likely to affect the transduction of auditory signals by IHC. Sound-induced movements are detected by stereocilia which pivot at their tapered bottom ends. Deflections alter the tension on "tip-links" that run between the tip of each shorter stereocilum to the shaft the longer stereocilium behind to open and close the mechanotransduction (MET) channels located at the tips of each of the shorter stereocilium, thereby modulating a K^+ current through the hair cell and its electrical potential (Fettiplace, 2017). Fusion of stereocilia will likely result in reduced bundle movement due to loss of the taper and increased rigidity of the fused stereocilia due to the incorporation of multiple actin cores. In addition, tip-links will be lost and the number and/or distribution of MET channels may be affected. The result will be loss of signal transduction and the fidelity of sound transmission to the auditory nerve. However, the initial effects of a reduction of the neural output from individual IHC scattered along the organ of Corti to recordable measures of auditory acuity is likely to be subtle and difficult to identify by current methods.

The persistence of stereocilary abnormalities on IHC, coupled with the absence of indications of damage or degeneration within the body of the IHC indicate the likelihood of an age-related pathology affecting the hair bundles specifically: a "stereociliopathy". The stereocilial abnormalities shown in this study are similar to the fusion and elongation of vestibular hair cells described previously (Taylor et al., 2015). This supports the concept that there is a general vulnerability of hair bundle maintenance to the effects of ageing in the inner ear. However, while IHCs and vestibular hair cells were strongly affected in both humans and mice, OHCs were not seen to be affected in mice or other rodents (Coleman, 1976; Keithley and Feldman, 1982; Tarnowski et al., 1991) and there were very few

examples of fused stereocilia in OHCs of human samples. This may indicate stereocilial maintenance or deterioration mechanisms vary between different hair cell types.

TEM and the electron tomography show that the paracrystalline arrays of parallel actin filaments are undisturbed when fusion occurs – they do not break, disassemble or re-associate with each other. Thus, while the increase in width in fused and giant, elongated stereocilia that subsequently develop is likely a result of accumulation of the existing filaments into the fusing stereocilia, the increase in length is presumably due to growth of the actin filaments. Stereocilia grow in length during development by addition of actin monomers to the apical tips of the filaments and are maintained during life by a slow turnover of actin in a small compartment at that tip (Drummond et al., 2015; McGrath et al., 2017; Narayanan et al., 2015; Pelaseyed and Bretscher, 2018). The elongation of stereocilia suggests therefore that the machinery for trafficking actin to the tips of stereocilia is still active, providing additional evidence for the “viability” of the hair cells upon which fused and elongated stereocilia are present. Normally, the precise length of each individual stereocilium is regulated and maintained by a complex of actin capping/depolymerising proteins that are localised to their apical tips (Olt et al., 2014; Peng et al., 2009; Zampini et al., 2011). The elongation of stereocilia that occurs would seem to imply that that regulation is lost, though whether this is because of an age-related reduction in the expression of the relevant proteins or a consequence of the effects of membrane fusions on their distribution or density would need to be assessed.

The electron tomography in this study provides evidence of detachment of the cuticular plate from the apical plasma membrane to form a “gap” of cytoplasm between the membrane and the cuticular plate and the “zipping-up” of detached apical membrane from the base to the tip of the stereocilium to incorporate adjacent bundles into a single fused projection. A similar mechanism for formation of fused stereocilia was suggested in a previous study of ageing in vestibular sensory epithelia in mice and humans (Taylor et al., 2015). Membrane inclusions in the apical cytoplasmic space generated by separation of the cuticular plate from the

membrane could represent membrane elements trafficked during fusion of stereocilia, which will require membrane remodelling. The role of the microtubules revealed by electron tomography in this region is not known, but may be related to trafficking of components to or from fusing stereocilia. Vesicles were often present in the cell body region close to the location of internalised actin filament bundles and within the gap that developed between the apical plasma membrane and the cuticular plate, particularly in cells with internalised stereocilia. These vesicles were not seen in younger mice. Many of these vesicles appeared to be double-membraned and similar to autophagic vesicles. This may suggest the actin filaments and other components of the re-modelling hair bundle are removed by autophagy. Autophagy acts to remove damaged or excess cellular material enabling the components to be recycled in support of continuing cellular metabolism and synthesis and is upregulated in times of cellular stress, for example to provide energy sources when cells are starved (and the huge actin content in resorbed stereocilia would make a substantial meal) (Rubinsztein et al., 2011). We have evidence elsewhere that the autophagic flux in IHC is much greater than that in OHC (Taylor and Forge in preparation) and it is possible that autophagy plays a role in the prolonged survival of IHC during ageing.

The stereociliopathy observed with ageing is similar to that described in a number of conditions thought to result from a defect in the maintenance of actin-cytoskeletal interactions. Fusion and internalisation of stereocilia and separation of the cuticular plate from the apical plasma membrane of the hair cell has been observed in mice lacking radixin (Kitajiri et al., 2004), one of the “ERM proteins” (ezrin/radixin/moesin) that act to link actin filaments to the plasma membrane (Fievet et al., 2007). The phenotype develops first in young adults and then progresses but does not result in hair cell loss. Similar stereociliary anomalies are seen in the early postnatal organ of Corti exposed to staurosporine which causes loss of phosphorylated forms of ERM proteins (Goodyear et al., 2014). Mutations in the gene encoding myosin 6 also result in fusion and elongation of stereocilia in mice (Self et

al., 1999). Here again, the hair bundles show normal characteristics at birth but fusion and elongation occurs subsequently and then progresses in severity and extent into adulthood without any hair cell death occurring. In all these cases, the fusion and internalisation of stereocilia appears to occur through detachment and separation of the apical plasma membrane from the cuticular plate and a “zipping-up” of the membrane between the adjacent stereocilia along its length from base to tip, similar to that observed for fusion of stereocilia in the present work. Neither loss of radixin or staurosporine treatment caused hair cell death, and their effects appeared to be specific to the hair bundle. However, both loss of radixin and staurosporine exposure cause apparently similar effects on both IHC and OHC, but radixin loss affects only cochlear hair cells and not those of the vestibular system (Kitajiri et al., 2004). Myosin 6 may have several roles in the hair cell, but the finding of apical membrane detachment in the early stages of the fusion process suggested the likelihood that myosin 6 acts to anchor the apical plasma membrane to the cuticular plate and possibly also maintain membrane domain composition.

Stereocilia fusion and elongation are also associated with mutations in PTPRQ, a receptor-like inositol lipid phosphatase, required for formation during development of “shaft connectors” that form links between the membranes of adjacent stereocilia. Its absence results in fused elongated stereocilia in IHC of the mature organ of Corti (Goodyear et al., 2003). It could be hypothesised that fusion occurs when membranes of adjacent stereocilia to come into contact and that loss of PTPRQ and consequently shaft connectors might therefore facilitate fusion. However, loss of shaft connectors in *PTPRQ* mutants does not lead to direct contact of adjacent stereocilia (Goodyear et al., 2003). PTPRQ may act to regulate and maintain local inositol phosphoinositide phospholipid composition, in turn regulating rates of membrane and actin turnover. Consequently, loss of PTPRQ would result in failure to maintain stereociliary membrane domain composition and associated membrane-cytoskeletal interactions, facilitating fusion events. There is evidence that there

526 are differences between hair cell types in their susceptibility to loss of PTPRQ possibly
527 because in some hair cell types other phosphatases can compensate for its loss (Goodyear
528 et al., 2003). This could be a factor underlying the observed difference between IHC and
529 OHC in age-related stereociliary “fusion-competence”.

530 Although the molecular and biochemical mechanisms at work during the age-related
531 stereociliopathy are not clear, similarities with the effects of inactivation of ERM proteins,
532 loss of myosin 6, and *PTPRQ* mutations, indicate that an age-related failure to maintain
533 regulation of membrane turnover and membrane-cytoskeletal interactions within the
534 stereocilia may be a significant factor in stereociliopathy. The stereociliopathies described
535 here appeared scattered along the cochlear spiral, although there was some evidence that
536 giant stereocilia may be more common at the apex of the cochlea compared to the base.
537 The reason for this potential apex to base gradient is not clear, although it may indicate
538 differences in stereocilial maintenance and actin turnover along the length of the cochlea.

539

540 **Tectorial membrane degeneration.**

541 In addition to stereociliopathy, age-related degradation of the tectorial membrane has also
542 been identified in this study as a potential contributor to hearing deficits in humans. Recent
543 work has shown a similar TM phenotype in aging of several wild-type mouse strains, and
544 indicated that the severity of aging phenotype may be genetically determined (Goodyear,
545 2019). The TM performs several tasks (Goodyear and Richardson, 2018; Lukashkin et al.,
546 2010), but primarily maximises the sound induced movement that deflects IHC stereocilia at
547 their best or characteristic frequency. The TM is therefore responsible for enhancing both
548 auditory sensitivity and frequency selectivity. TM function depends upon its physical
549 properties, its mass and its stiffness, both of which vary systematically along the cochlea:
550 mass increases from base to apex; stiffness increases apex to base (Goodyear and
551 Richardson, 2018; Teudt and Richter, 2014). Our study reveals in mice a progressive

552 degeneration of the TM that will affect its physical properties, proceeding with increasing age
553 from the apical coils towards the base. This is apparent initially as a progressive loss of the
554 striated-sheet matrix and the two major glycoproteins of which it composed, TECTA and
555 TECTB (Goodyear and Richardson, 2018), that proceeds from the central regions of the
556 membrane towards the periphery. “Holes” appear in the body of TM and there is a
557 subsequent decrease in density of the radial collagen fibrils, such that in some of the oldest
558 animals the TM may appear as little more than an “exoskeleton” surrounding a significantly
559 reduced density of collagen fibrils. Beginning in the apical coil, the TM separates from the
560 spiral limbus eventually detaching completely and becoming associated with the
561 endolymphatic side of Reissner’s membrane. During the progressive degeneration TM
562 shape changes, sometimes appearing thinned and sometimes apparently swollen. Changes
563 in the shape of the TM suggesting changes in composition, in particular thinning of the
564 membrane, as well as evidence of separation from the spiral limbus and close association or
565 attachment with the Reissner’s membrane, were also evident in the cochleae of elderly
566 human subjects. Although the tectorial membrane remained in proximity to the hair cells at
567 the very apex of the human cochleae studied, the thinning and attachment to Reissner’s
568 membrane were most pronounced in the apical and middle coils, suggesting the possibility
569 that an age-related apical to basal progression of TM disruption along the organ of Corti,
570 similar to that seen in mice, may also occur in humans.

571 TECTA and TECTB are produced only for a short time during early development (Rau et al.,
572 1999), and the matrix is not replenished during life. CEACAM16, which interacts with both
573 TECTA and TECTB and is required for striated-sheet formation, is produced throughout life.
574 (Cheatham et al., 2014). Targeted deletion of the genes encoding TECTA (*Tecta*) (Legan et
575 al., 2000), and TECTB (*Tectb*) (Russell et al., 2007) induces loss of the striated sheet matrix
576 and hearing impairment, without any effects on hair cells. Non-syndromic autosomal hearing
577 loss in humans results from point mutations in the human homologue for TECTA (*TECTA*)
578 that are either dominant (DFNA8/12) or recessive (DFNB21) and likewise for *CEACAM16*

(DFNA4b and DFNB113). With loss of TECTA, TECTB is also lost. Morphologically, the TM appears less dense than normal, its shape is disrupted and it separates from the spiral limbus, detaching completely to become closely associated with Reissner's membrane. Point mutations in *Tecta* in mice cause elevation of auditory thresholds, although the different mutations result in distinctive disruptions of particular details of TM structure. Shape changes and reduction in the zone of attachment with the spiral limbus were common features, and in some the reduced TECTB expression and advanced detachment of the TM were particularly pronounced in apical coils (Legan et al., 2014). Loss of TECTB also results in loss of the striated sheet matrix, and large changes in TM cross-sectional profile in the apical coil causing a loss of low-frequency hearing. However TECTA is still expressed in the *Tectb*$^{-/-}$ mice and the TM does not detach from the spiral limbus. Detailed analysis of the biophysical and physiological consequences of loss of TECTB suggests it is essential for low frequency hearing (Russell et al., 2007). Levels of TECTB, but not of TECTA, are slightly reduced in the TM of mice carrying a targeted null mutation in *Ceacam16*. In these mice, the TM remains attached to spiral limbus, but there are "holes" within the body of the TM that are most pronounced in the apical coils (Cheatham et al., 2014) and similar to those seen in the much older wild type mice used in the current study. Recent work has also shown that CEACAM16 is required to maintain the TM structure during aging, and that its absence produces an accelerated aging phenotype (Goodyear, 2019).

It is also possible that an age-related reduction in endocochlear potential (EP) and degeneration of the stria vascularis may affect TM structure. The TM is sensitive to its ionic environment, particularly calcium concentration (Goodyear and Richardson, 2018; Strimbu et al., 2019). However, the stria vascularis is primarily responsible for maintaining potassium ions and EP (Salt et al., 1987), and how this affects overall ion balance in endolymph is not clear. It is therefore difficult to speculate on whether there are changes in the ionic environment of the endolymph in which the TM is bathed contribute in any way to the degeneration observed, and this was not studied in these experiments.

Therefore, it is possible to hypothesise two scenarios leading to the age related degeneration of the tectorial membrane. Both immunohistochemistry and the detachment of the TM from the spiral limbus in both mice and humans strongly suggests that loss of TECTA is a significant factor in age-related TM degradation. This could suggest that tectorins are the principle target of degradation, as these proteins are not replenished throughout life. A second hypothesis is that CEACAM16 acts as a stabiliser for the tectorin proteins in the striated sheet matrix, and it is a reduction or dysregulation of the production of this protein with ageing that leads to degradation of the matrix and loss of the tectorin proteins. Late onset hearing loss is also present in humans with mutations in CEACAM16 (DFNB113) indicating that this may be an important factor in age-related TM degradation and hearing loss (Goodyear, 2019).

This study was limited in its human data by the limited number of samples of sufficient quality and with appropriate medical history that could be included (i.e. the presence or known absence of presbycusis in the older samples). However, despite this we were able to demonstrate stereocilial fusion phenotypes in both sexes, although we only had suitable tectorial membrane examples from males. Due to these limitations, it is difficult to say if there were any sex differences between the samples as sample numbers are not sufficient. In the mouse studies, male mice were used exclusively, to avoid confounding factors from the different rates of ARHL between the sexes (Guimaraes et al., 2004). This does mean the study is limited in examining the potential sex differences in these phenotypes. Such differences may well exist, given the differing rates of ARHL between the sexes in mice, and the description of these phenotypes in this study could form the basis of a future examination of this question.

Age-related increases of auditory thresholds, are typically reported as beginning at high frequencies progressing to involve successively lower frequencies, broadly corresponding to progressive loss of OHC proceeding from the basal coil apicalwards. Age-related synaptopathies are reported to occur in an apex to base pattern (Sergeyenko et al., 2013), similar to the patterns of stereociliopathy and TM degradation reported here. In particular, the pattern of occurrence of TM deterioration observed here suggests the likelihood of a low frequency component in the early stages of ARHL and which may be contributing to so-called “hidden hearing loss”. The continued deterioration progressing towards the base without obvious loss of hair cells could also suggest that TM degeneration contributes to age-related threshold elevations. The combination of all these factors are therefore likely to contribute to the early and later stages of age related hearing loss. This raises important questions for the development of future therapies, which must contend not only with hair cell loss and synaptopathy but also with hair cells that are present but whose function is impaired, and with the potential need to regenerate the TM. Therefore future therapeutic approaches may require a holistic approach to the organ of Corti and its surrounding structures to maximise their effectiveness.

Other Acknowledgements

Lucy Anderson for kindly providing some of the samples used in this study. Graham Nevill for technical assistance in sample preparation and Katie Smith for sample preparation and imaging.

Conflict of Interest Statement

Authors have no known conflicts of interest to declare.

Author Contributions

AB, AF and RT had full access to all the data in the study and take responsibility for the integrity of the data and the accuracy of the data analysis. Conceptualization: AB, AF, RG, GR, RT and TW. Methodology: AB, AF, RT and TW. Investigation: AB, AF, RT and TW Resources: AB, AF, RG, GR, RT and TW. Writing – Original Draft: AB, AF and RT. Writing – Review & Editing: AB, AF, RG, GR, RT and TW. Visualization: AB, AF. Funding Acquisition: AF, RT and AB.

Data Accessibility

Data available on request from the authors. Ethical and privacy restrictions may apply to human data.

References

Bao, J., and K.K. Ohlemiller. 2010. Age-related loss of spiral ganglion neurons. *Hear. Res.* 264:93-97.

Barbee, C.M., J.A. James, J.H. Park, E.M. Smith, C.E. Johnson, S. Clifton, and J.L. Danhauer. 2018. Effectiveness of Auditory Measures for Detecting Hidden Hearing Loss and/or Cochlear Synaptopathy: A Systematic Review. *Semin Hear*. 39:172-209.

Bullen, A. 2019. The Automatic Tape Collection UltraMicrotome (ATUM). *In* Biological Field Emission Scanning Electron Microscopy. R.A.H. Fleck, B. M., editor. WIley. 485-494.

Cheatham, M.A., R.J. Goodyear, K. Homma, P.K. Legan, J. Korchagina, S. Naskar, J.H. Siegel, P. Dallos, J. Zheng, and G.P. Richardson. 2014. Loss of the tectorial membrane protein CEACAM16 enhances spontaneous, stimulus-frequency, and transiently evoked otoacoustic emissions. *J. Neurosci.* 34:10325-10338.

Coleman, J.W. 1976. Hair Cell Loss as a Function of Age in the Normal Cochlea of the Guinea Pig. *Acta Otolaryngol.* 82:33-40.

Davies, S., and A. Forge. 1987. Preparation of the mammalian organ of Corti for scanning electron microscopy. *J. Microsc.* 147:89-101.

Davis, A. 1995. Hearing in Adults: The prevalence and distribution of hearing impairment and reported hearing disability in the MRC Institute of Hearing Research's National Study of Hearing. Whurr Publishers Ltd. , London.

Drummond, M.C., M. Barzik, J.E. Bird, D.S. Zhang, C.P. Lechene, D.P. Corey, L.L. Cunningham, and T.B. Friedman. 2015. Live-cell imaging of actin dynamics reveals mechanisms of stereocilia length regulation in the inner ear. *Nat Commun*. 6:6873.

Engle, J.R., S. Tinling, and G.H. Recanzone. 2013. Age-related hearing loss in rhesus monkeys is correlated with cochlear histopathologies. *PloS One*. 8:e55092.

Fettiplace, R. 2017. Hair Cell Transduction, Tuning, and Synaptic Transmission in the Mammalian Cochlea. *Compr Physiol*. 7:1197-1227.

Fievet, B., D. Louvard, and M. Arpin. 2007. ERM proteins in epithelial cell organization and functions. *Biochim. Biophys. Acta*. 1773:653-660.

Gleich, O., P. Semmler, and J. Strutz. 2016. Behavioral auditory thresholds and loss of ribbon synapses at inner hair cells in aged gerbils. *Exp. Gerontol.* 84:61-70.

Goodyear, R.J., Cheatham, M.A., Naskar, S., Zhou, Y., Osgood, R.T., Zheng, J., Richardson, G.P. 2019. Accelerated Age-Related Degradation of the Tectorial Membrane in the Ceacam16 beta-gal/beta-gal Null Mutant Mouse, A Model for Late-

703 Onset Human Hereditary Deafness DFNB113. *Frontiers in Molecular Neuroscience*.
704 12:147.
705 Goodyear, R.J., P.K. Legan, M.B. Wright, W. Marcotti, A. Oganesian, S.A. Coats, C.J.
706 Booth, C.J. Kros, R.A. Seifert, D.F. Bowen-Pope, and G.P. Richardson. 2003. A
707 receptor-like inositol lipid phosphatase is required for the maturation of developing
708 cochlear hair bundles. *J. Neurosci.* 23:9208-9219.
709 Goodyear, R.J., H.S. Ratnayaka, M.E. Warchol, and G.P. Richardson. 2014. Staurosporine-
710 induced collapse of cochlear hair bundles. *J. Comp. Neurol.* 522:3281-3294.
711 Goodyear, R.J., and G.P. Richardson. 2002. Extracellular matrices associated with the
712 apical surfaces of sensory epithelia in the inner ear: molecular and structural
713 diversity. *J. Neurobiol.* 53:212-227.
714 Goodyear, R.J., and G.P. Richardson. 2018. Structure, Function, and Development of the
715 Tectorial Membrane: An Extracellular Matrix Essential for Hearing. *Curr. Top. Dev.*
716 *Biol.* 130:217-244.
717 Gratton, M.A., R.A. Schmiedt, and B.A. Schulte. 1996. Age-related decreases in
718 endocochlear potential are associated with vascular abnormalities in the stria
719 vascularis. *Hear. Res.* 102:181-190.
720 Guimaraes, P., X. Zhu, T. Cannon, S. Kim, and R.D. Frisina. 2004. Sex differences in
721 distortion product otoacoustic emissions as a function of age in CBA mice. *Hear.*
722 *Res.* 192:83-89.
723 Hasko, J.A., and G.P. Richardson. 1988. The ultrastructural organization and properties of
724 the mouse tectorial membrane matrix. *Hear. Res.* 35:21-38.
725 Hequembourg, S., and M.C. Liberman. 2001. Spiral ligament pathology: a major aspect of
726 age-related cochlear degeneration in C57BL/6 mice. *J Assoc Res Otolaryngol*. 2:118-
727 129.
728 Ichimiya, I., M. Suzuki, and G. Mogi. 2000. Age-related changes in the murine cochlear
729 lateral wall. *Hear. Res.* 139:116-122.
730 Keithley, E.M., and M.L. Feldman. 1982. Hair cell counts in an age-graded series of rat
731 cochleas. *Hear. Res.* 8:249-262.
732 Kitajiri, S., K. Fukumoto, M. Hata, H. Sasaki, T. Katsuno, T. Nakagawa, J. Ito, S. Tsukita,
733 and S. Tsukita. 2004. Radixin deficiency causes deafness associated with
734 progressive degeneration of cochlear stereocilia. *J. Cell Biol.* 166:559-570.
735 Knipper, M., G. Richardson, A. Mack, M. Muller, R. Goodyear, A. Limberger, K. Rohbock, I.
736 Kopschall, H.P. Zenner, and U. Zimmermann. 2001. Thyroid hormone-deficient
737 period prior to the onset of hearing is associated with reduced levels of beta-tectorin
738 protein in the tectorial membrane: implication for hearing loss. *J. Biol. Chem.*
739 276:39046-39052.
740 Kremer, J.R., D.N. Mastronarde, and J.R. McIntosh. 1996. Computer visualization of three-
741 dimensional image data using IMOD. *J. Struct. Biol.* 116:71-76.
742 Kujawa, S.G., and M.C. Liberman. 2015. Synaptopathy in the noise-exposed and aging
743 cochlea: Primary neural degeneration in acquired sensorineural hearing loss. *Hear.*
744 *Res.* 330:191-199.
745 Kusunoki, T., S. Cureoglu, P.A. Schachern, K. Baba, S. Kariya, and M.M. Paparella. 2004.
746 Age-Related Histopathologic Changes in the Human Cochlea: A Temporal Bone
747 Study. *Otolaryngology–Head and Neck Surgery*. 131:897-903.
748 Legan, P.K., R.J. Goodyear, M. Morin, A. Mencia, H. Pollard, L. Olavarrieta, J. Korchagina,
749 S. Modamio-Hoybjor, F. Mayo, F. Moreno, M.A. Moreno-Pelayo, and G.P.
750 Richardson. 2014. Three deaf mice: mouse models for TECTA-based human
751 hereditary deafness reveal domain-specific structural phenotypes in the tectorial
752 membrane. *Hum. Mol. Genet.* 23:2551-2568.
753 Legan, P.K., V.A. Lukashkina, R.J. Goodyear, M. Kossi, I.J. Russell, and G.P. Richardson.
754 2000. A targeted deletion in alpha-tectorin reveals that the tectorial membrane is
755 required for the gain and timing of cochlear feedback. *Neuron*. 28:273-285.
756 Lukashkin, A.N., G.P. Richardson, and I.J. Russell. 2010. Multiple roles for the tectorial
757 membrane in the active cochlea. *Hear. Res.* 266:26-35.

McGrath, J., P. Roy, and B.J. Perrin. 2017. Stereocilia morphogenesis and maintenance through regulation of actin stability. *Semin Cell Dev Biol*. 65:88-95.
Narayanan, P., P. Chatterton, A. Ikeda, S. Ikeda, D.P. Corey, J.M. Ervasti, and B.J. Perrin. 2015. Length regulation of mechanosensitive stereocilia depends on very slow actin dynamics and filament-severing proteins. *Nat Commun*. 6:6855.
Olt, J., P. Mburu, S.L. Johnson, A. Parker, S. Kuhn, M. Bowl, W. Marcotti, and S.D.M. Brown. 2014. The Actin-Binding Proteins Eps8 and Gelsolin Have Complementary Roles in Regulating the Growth and Stability of Mechanosensory Hair Bundles of Mammalian Cochlear Outer Hair Cells. *Plos One*. 9.
Parthasarathy, A., and S.G. Kujawa. 2018. Synaptopathy in the Aging Cochlea: Characterizing Early-Neural Deficits in Auditory Temporal Envelope Processing. *J. Neurosci.* 38:7108-7119.
Pelaseyed, T., and A. Bretscher. 2018. Regulation of actin-based apical structures on epithelial cells. *J. Cell Sci.* 131.
Peng, A.W., I.A. Belyantseva, P.D. Hsu, T.B. Friedman, and S. Heller. 2009. Twinfilin 2 regulates actin filament lengths in cochlear stereocilia. *J. Neurosci.* 29:15083-15088.
Rau, A., P.K. Legan, and G.P. Richardson. 1999. Tectorin mRNA expression is spatially and temporally restricted during mouse inner ear development. *J. Comp. Neurol.* 405:271-280.
Rauch, S.D., L. Velazquez-Villasenor, P.S. Dimitri, and S.N. Merchant. 2001. Decreasing hair cell counts in aging humans. *Ann. N. Y. Acad. Sci.* 942:220-227.
Rubinsztein, D.C., G. Marino, and G. Kroemer. 2011. Autophagy and aging. *Cell*. 146:682-695.
Russell, I.J., P.K. Legan, V.A. Lukashkina, A.N. Lukashkin, R.J. Goodyear, and G.P. Richardson. 2007. Sharpened cochlear tuning in a mouse with a genetically modified tectorial membrane. *Nature neuroscience*. 10:215-223.
Salt, A.N., I. Melichar, and R. Thalmann. 1987. Mechanisms of endocochlear potential generation by stria vascularis. *Laryngoscope*. 97:984-991.
Schmiedt, R.A. 1996. Effects of aging on potassium homeostasis and the endocochlear potential in the gerbil cochlea. *Hear. Res.* 102:125-132.
Schmiedt, R.A., J.H. Mills, and F.A. Boettcher. 1996. Age-related loss of activity of auditory-nerve fibers. *J. Neurophysiol.* 76:2799-2803.
Self, T., T. Sobe, N.G. Copeland, N.A. Jenkins, K.B. Avraham, and K.P. Steel. 1999. Role of myosin VI in the differentiation of cochlear hair cells. *Dev. Biol.* 214:331-341.
Sergeyenko, Y., K. Lall, M.C. Liberman, and S.G. Kujawa. 2013. Age-related cochlear synaptopathy: an early-onset contributor to auditory functional decline. *J. Neurosci.* 33:13686-13694.
Strimbu, C.E., S. Prasad, P. Hakizimana, and A. Fridberger. 2019. Control of hearing sensitivity by tectorial membrane calcium. *Proc Natl Acad Sci U S A*. 116:5756-5764.
Suzuki, T., Y. Nomoto, T. Nakagawa, N. Kuwahata, H. Ogawa, Y. Suzuki, J. Ito, and K. Omori. 2006. Age-Dependent Degeneration of the Stria Vascularis in Human Cochleae. *The Laryngoscope*. 116:1846-1850.
Tarnowski, B.I., R.A. Schmiedt, L.I. Hellstrom, F.S. Lee, and J.C. Adams. 1991. Age-related changes in cochleas of mongolian gerbils. *Hear. Res.* 54:123-134.
Taylor, R.R., D.J. Jagger, S.R. Saeed, P. Axon, N. Donnelly, J. Tysome, D. Moffatt, R. Irving, P. Monksfield, C. Coulson, S.R. Freeman, S.K. Lloyd, and A. Forge. 2015. Characterizing human vestibular sensory epithelia for experimental studies: new hair bundles on old tissue and implications for therapeutic interventions in ageing. *Neurobiol. Aging*. 36:2068-2084.
Teudt, I.U., and C.P. Richter. 2014. Basilar membrane and tectorial membrane stiffness in the CBA/CaJ mouse. *J Assoc Res Otolaryngol*. 15:675-694.
Thomopoulos, G.N., S.S. Spicer, M.A. Gratton, and B.A. Schulte. 1997. Age-related thickening of basement membrane in stria vascularis capillaries. *Hear. Res.* 111:31-41.

812 Wright, A. 1982. Giant cilia in the human organ of Corti. *Clin Otolaryngol Allied Sci*. 7:193-
813 199.
814 Wright, A. 1984. Dimensions of the cochlear stereocilia in man and the guinea pig. *Hear.*
815 *Res.* 13:89-98.
816 Wright, A., A. Davis, G. Bredberg, L. Ulehlova, and H. Spencer. 1987. Hair cell distributions
817 in the normal human cochlea. *Acta Otolaryngol. Suppl.* 444:1-48.
818 Wu, P.Z., L.D. Liberman, K. Bennett, V. de Gruttola, J.T. O'Malley, and M.C. Liberman.
819 2018. Primary Neural Degeneration in the Human Cochlea: Evidence for Hidden
820 Hearing Loss in the Aging Ear. *Neuroscience*.
821 Yamasoba, T., S. Someya, C. Yamada, R. Weindruch, T.A. Prolla, and M. Tanokura. 2007.
822 Role of mitochondrial dysfunction and mitochondrial DNA mutations in age-related
823 hearing loss. *Hear. Res.* 226:185-193.
824 Zampini, V., L. Ruttiger, S.L. Johnson, C. Franz, D.N. Furness, J. Waldhaus, H. Xiong, C.M.
825 Hackney, M.C. Holley, N. Offenhauser, P.P. Di Fiore, M. Knipper, S. Masetto, and W.
826 Marcotti. 2011. Eps8 regulates hair bundle length and functional maturation of
827 mammalian auditory hair cells. *PLoS Biol*. 9:e1001048.
828 Zheng, J., K.K. Miller, T. Yang, M.S. Hildebrand, A.E. Shearer, A.P. DeLuca, T.E. Scheetz,
829 J. Drummond, S.E. Scherer, P.K. Legan, R.J. Goodyear, G.P. Richardson, M.A.
830 Cheatham, R.J. Smith, and P. Dallos. 2011. Carcinoembryonic antigen-related cell
831 adhesion molecule 16 interacts with alpha-tectorin and is mutated in autosomal
832 dominant hearing loss (DFNA4). *Proc Natl Acad Sci U S A*. 108:4218-4223.

833

834 **Figure legends**

835

836 **Figure 1. Stereocilia fusion, elongation and internalisation in ageing mice cochleae**

837 (a) ABR thresholds in an ageing cohort of CBA/Ca mice. Threshold increases at both the
838 high and low frequency regions are evident at 18 and 24 months. Error bars represent
839 Standard Error of the Mean (SEM). Animals per group: 6 months (n=20), 12 months (n=16),
840 18 months (n=11) and 24 months (n=6). P-values for repeated measures ANOVA (Click
841 P=0.01, df=1.416. 8kHz P=0.042, df=3. 12kHz P=0.025, df=3. 24kHz P=<0.001, df=3.
842 P=<0.001, df=3. 32kHz P=<0.001, df=3. 40kHz P=0.004, df=3. (b) Middle coil and (c) Basal
843 coil from a 6 month mouse. No evidence of inner or outer hair cell damage is present. (d-f)
844 Middle coil in (d) 12 month, (e) 18 month and (f) 24 month mice. Stereocilial fusions and
845 internalisation are present in all three (white arrows); both fusion and lost hair cells (*) are
846 more prevalent at older ages. Boxed region in (d) represents an enlargement of the
847 stereocilial fusion defined by the arrow. (g-i) (g) Apical, (h) Middle and (i) Basal coils of
848 mouse cochleae at 24 months of age. Fusions and hair cell loss are most severe in the
849 apical region. (j-l) Stereocilial defects in 24 month mice. (j) Severe stereocilial fusions and

internalisation. (k) Elongation of stereocilium. (l) Fusion across longest stereocilial row. Scale bars (b-i and k) 10μm, (j and l) 1μm.

Figure 2. Stereocilia fusion, elongation and internalisation in aged human cochleae

All cochleae were from people who had no recorded hearing loss at time of death. (a-c): apical middle and basal cochlear turns from 26 year old female. Irregularity in the rows, presence of a 4th row of OHC in (c), and supernumerary OHC and IHC are evident, these are characteristic of the normal human organ of Corti. Scattered loss of IHC is indicated by (*), but stereocilial defects were not observed. (d-i): evidence of fusion and elongation (white arrows) and internalisation (red arrows and insets) in (d) a 62 year old male, (e) a 69 year old male and (f) a 60 year old female. (g) Fusion, elongation and engulfment of OHC stereocilia in a 69 year old male. Fusion of OHC stereocilia was not observed in mice. (h and i) Comparison of fused, elongated stereocilia in human (h, 77 year old male) and mouse (i, 30 months). Scale bars: a-c and g = 10μm, d, e, h-i = 1μm (inset 1μm), f = 2μm (insets 2μm).

Figure 3. Stereocilia fusion, elongation and internalisation in aged mouse and human vestibular tissue

(a) Mouse utricular macula at 18 months. (b) mouse utricular macula at 24 months. (c) mouse crista at 24 months. (d,e) Human utricular macula: Male, 70 years (d); Male 65 (e). Arrows indicate fused stereocilia, elongation of stereocilia and internalisation of stereocilia. In mouse, fusion of stereocilia is apparent before any significant hair cell loss, as indicated by close packing and high density of hair cells (a). Fused and elongated stereocilia persist in utricular maculae (b) and cristae (c) for at least 24 months by which time there is also a reduced density of hair cells. Internalisation of stereocilia (red arrows) (d) as well as

stereociliary fusion (e) are also features of the utricular macula in ageing humans. Scale bars: (a) 10um, (b-e) 1um.

Figure 4. Cross sectional examination of fused stereocilia bundles

(a-e) TEM cross sections of IHCs carrying fused or internalised stereocilia. (a-b) Stereocilial fusions (black arrows) on IHCs from mice aged 18 months. Despite the fusions the cell bodies appear normal and surrounding structures are not apparently impaired. Asterisks on enlarged insets in a and d indicate intact afferent terminals synapsing with the IHC. (c) Internalisation of stereocilia by the apical membrane (black arrow), 24 month mouse. (d-e) Internalisation of stereocilia (black arrows) in (d) 30 month and (e) 24 month mouse. In both cases the cell bodies and surrounding structures do not appear damaged. Insets show vesicles present in the cytoplasm near the sites of internalisation. These vesicles appear double walled, and to have contents. (f) Central section of tomographic reconstruction of fused IHC stereocilia. (g) Segmented reconstruction of stereocilial fusion. Manual segmentation was used for membranes and microtubules, actin filaments were rendered by isosurface rendering. Light blue = cell membrane Green = Stereocilial actin Red = Microtubules Purple and Blue = Membranous spheres without apparent contents (large and small respectively). Orange = membranous spheres with cytoplasmic contents. White = tubular cisternae. Brown= Isosurface rendering of cuticular plate. (h) Enlarged regions of central slice of tomographic reconstruction showing (i) stereocilial fusion tip with continuous membrane and actin filaments. (ii) Central shafts of stereocilial fusion with gaps between adjacent stereocilia and actin bundles, membrane fusion and central stereocilial rootlet. (iii) Cytoskeletal elements and membranous objects at the base of the stereocilial fusion. (iv) Individual stereocilium not included in fusion, showing similar actin pattern. (j) Enlargements from segmentation showing (i) Pattern of actin isosurface for complete 3D reconstruction of stereocilial fusion. (ii) Cytoskeletal and membrane components between fusion and cuticular plate. Scale bars a = 2μm (inset) = 1μm, b = 5 μm (inset = 500nm), c = 500nm, d (left) =

5μm (right) = 500nm (inset) = 500nm, e = 2μm, (inset) = 200nm, f-g = 250nm, h (i-iv) = 100nm, j (i, ii) = 200nm. For model rotations please see supplemental movie S1.

Figure 5. Light Microscopy of tectorial membrane degradation in cochleae of ageing mice and humans

(a-c) Tectorial membrane structure in mice. (a) 8 month old mouse showing no evidence of degradation in the tectorial membrane in any coil. (b) 22 month old mouse showing 'holes' in the membrane sheet, most severe in the apical coil and not present in the base (black arrows). (c) 30 month old mouse showing detachment of the tectorial membrane in the apical and middle coils, and evidence of detachment beginning in the basal coil (black arrows); holes in the membrane can also be seen in all three coils. Complete detachment from the spiral limbus and close association with Reissner's membrane is evident in the apical coil (d-f) Tectorial membrane structure in ageing humans. (d) Membrane from a 55 year old male with no recorded hearing loss. Membrane appears as a smooth sheet. (e) In an 81 year old male with reported presbycusis, membrane is thinned throughout the apical and middle coils. The membrane has detached to lie along Reissner's membrane in the apical and middle coils (black arrows). (f) A second male with presbycusis (71 years old) shows similar thinning of the membrane and attachment to Reissner's membrane. In the apical and middle coil the membrane has become attached to Reissner's membrane, while in the basal coil, although the membrane is not attached, extracellular material can be observed between the tectorial and Reissner's membranes. (Ap) Apical coil, (Ap/Mid) Apical to Middle coil, (Mi) Middle coil, (Ba) Basal coil. Scale Bars (a-f) = 50μm.

Figure 6. Tectorial membrane matrix degradation in ageing mice

(a-b) Backscatter imaging of resin sections showing middle turn in (a) 2 months and (b) 18 months mice. Tectorial membrane (white arrows) in (b) shows the same thinning and holes

apparent by light microscopy. The structure of the organ of Corti (OoC) shows no obvious defects and there is no obvious loss of cell bodies in the spiral ganglion (SG). (c-f) TEM imaging of tectorial membrane in 24 month old mice. (c) Very little striated sheet matrix remains leaving only the remains of the collagen skeleton. (d) In some samples although the matrix was lost, other structural elements around the periphery of the TM were intact. (e) Thinning of the membrane was also observed in mice. (f) High resolution shows the presence of collagen skeleton with loss of the matrix. (g-h) Electron tomography of the tectorial membrane in 2 month (g) and 12 month old mice (h). By 12 months, larger spaces are appearing in the striated sheet matrix, suggesting matrix material has been lost. Scale bars a-b = 50μm, c-e = 5μm, f = 500nm, g-h = 100nm. For model rotations see supplemental movies S2 and S3.

Figure 7. Immunohistochemistry of striated sheet matrix proteins in ageing mouse cochleae

Three striated sheet matrix proteins were stained by immunohistochemistry (green). (a) TECTA and TECTB labelling at 6 months in the mouse cochlear apex. Strong labelling is shown consistently across the tectorial membrane. (b) TECTA and TECTB labelling at 18 months in the apex and base of the mouse cochlea. At the apex, TECTA and TECTB has been lost from the centre of the tectorial membrane but persists at the periphery. At the base, staining for both proteins is consistent at 18 months and has just begun to fade at the centre for TECTB. (c) TECTA, TECTB and CEACAM16 labelling at the apex and base of the mouse cochlea at 24-30 months. All three proteins have been lost from the centre of the tectorial membrane in the cochlear apex. There is some evidence of loss of TECTA and TECTB in the centre of the tectorial membrane at the cochlear base, although CEACAM16 staining is more consistent. All samples were counterstained with phalloidin (magenta) to identify the actin in the organ of Corti. Scale bars 50μm.

Supporting Information

Supporting Movie S1 – Reconstruction and model of stereocilial fusion electron tomography from 1 year old mouse.

Supporting Movie S2 and S3 – Reconstruction and models of tectorial membrane matrix in 2 month and 12 month mice.

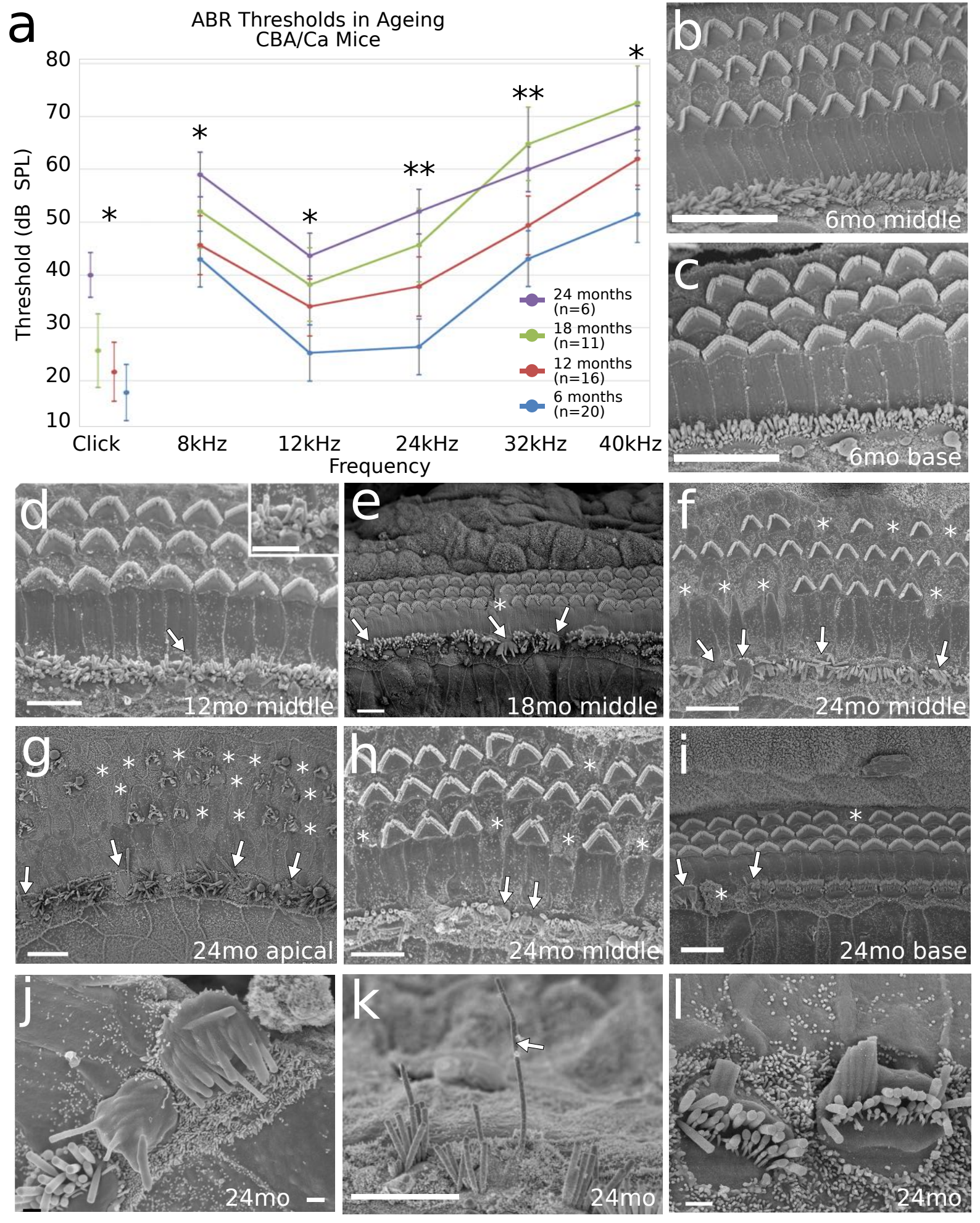
a
ABR Thresholds in Ageing
CBA/Ca Mice
Threshold (dB SPL)
80
70
60
50
40
30
20
10
Click
8kHz
12kHz
24kHz
32kHz
40kHz
Frequency
24 months (n=6)
18 months (n=11)
12 months (n=16)
6 months (n=20)
b
6mo middle
c
6mo base
d
12mo middle
e
18mo middle
f
24mo middle
g
24mo apical
h
24mo middle
i
24mo base
j
24mo
k
24mo
l
24mo

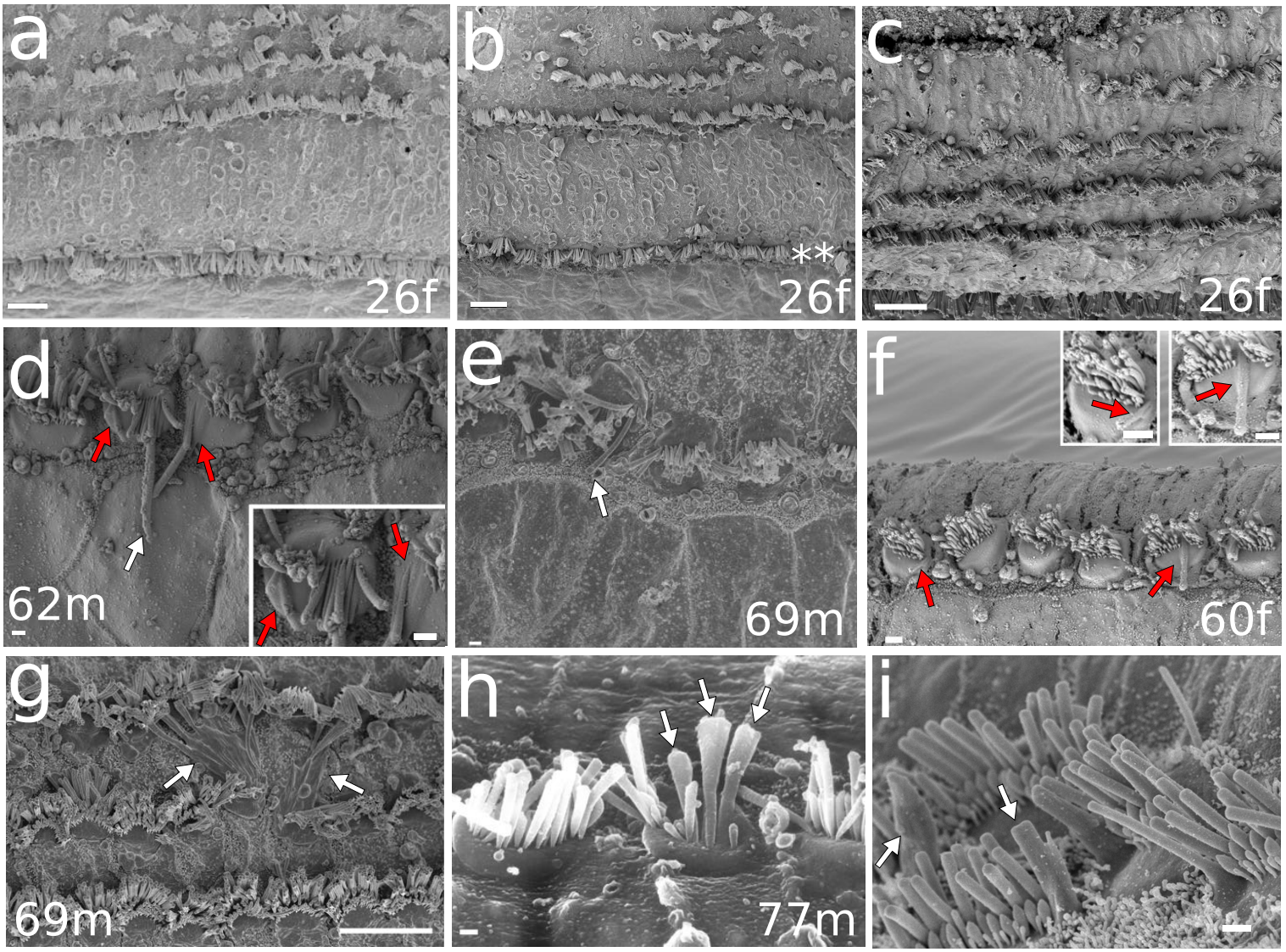
a
26f
b
**
26f
c
26f
d
62m
e
69m
f
60f
g
69m
h
77m
i

Mouse utricular macula

Mouse crista

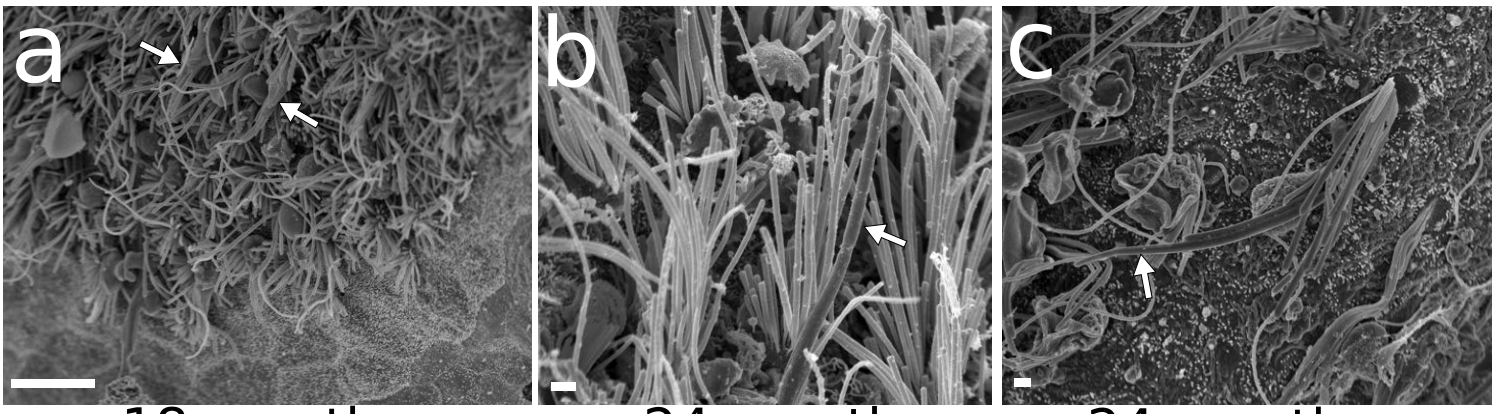

18 months

24 months

24 months

Human utricular macula

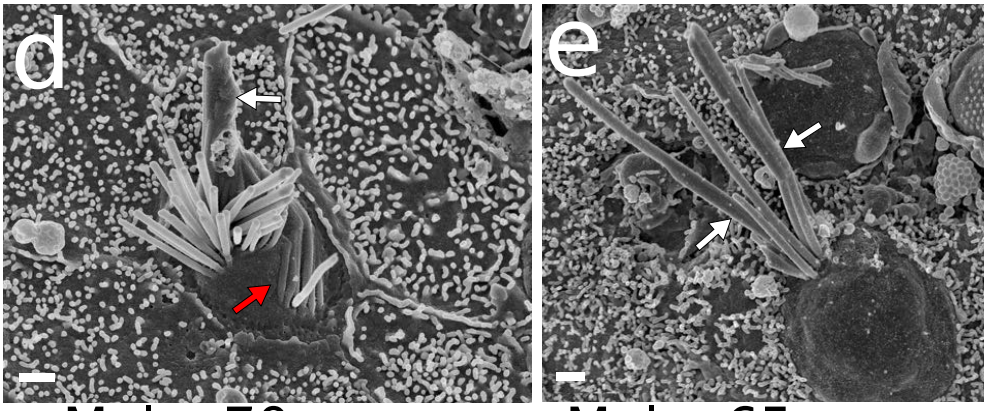

Male, 70 years

Male, 65 years

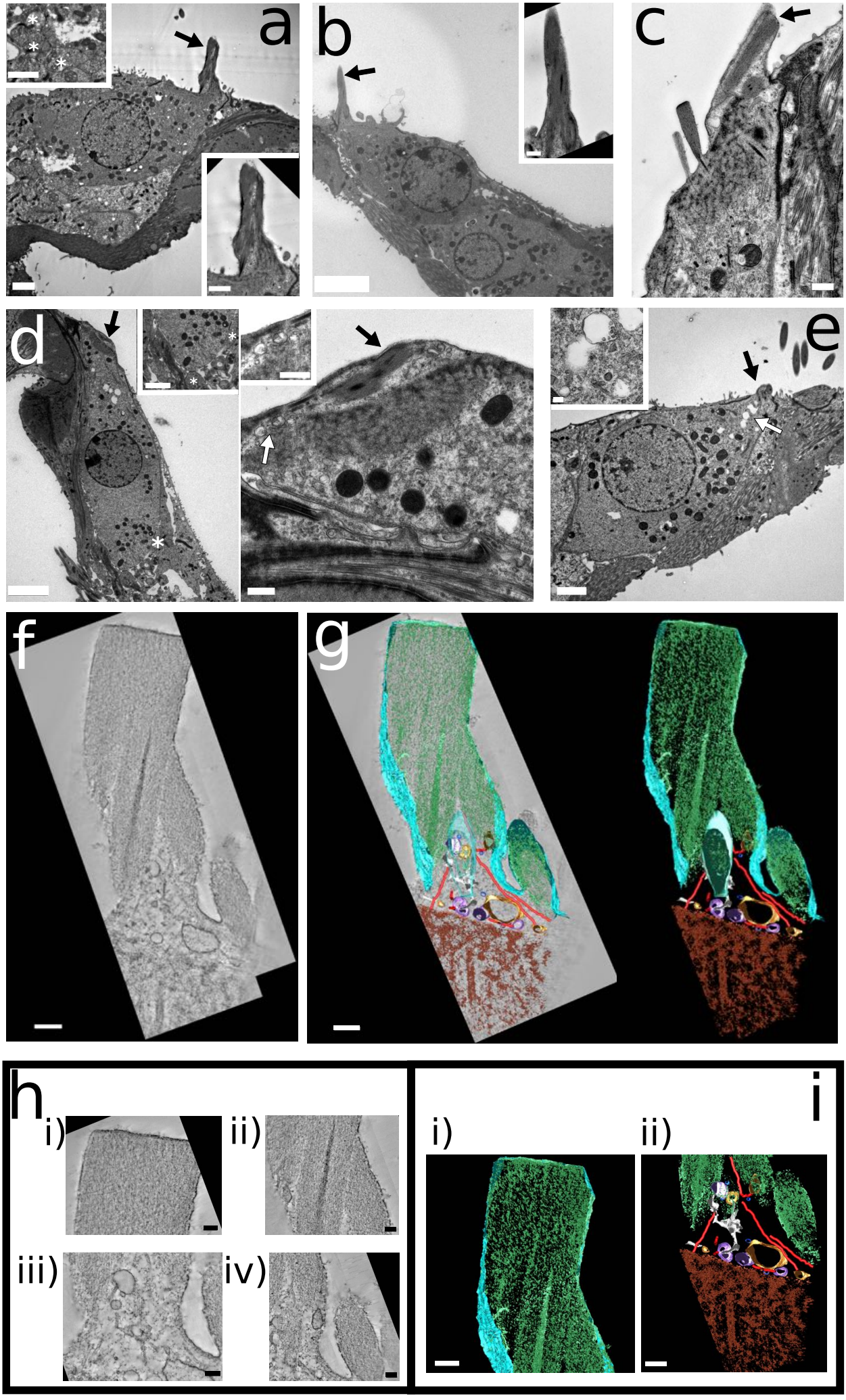
a
b
c
d
e
f
g
h
i)
ii)
iii)
iv)
i
i)
ii)

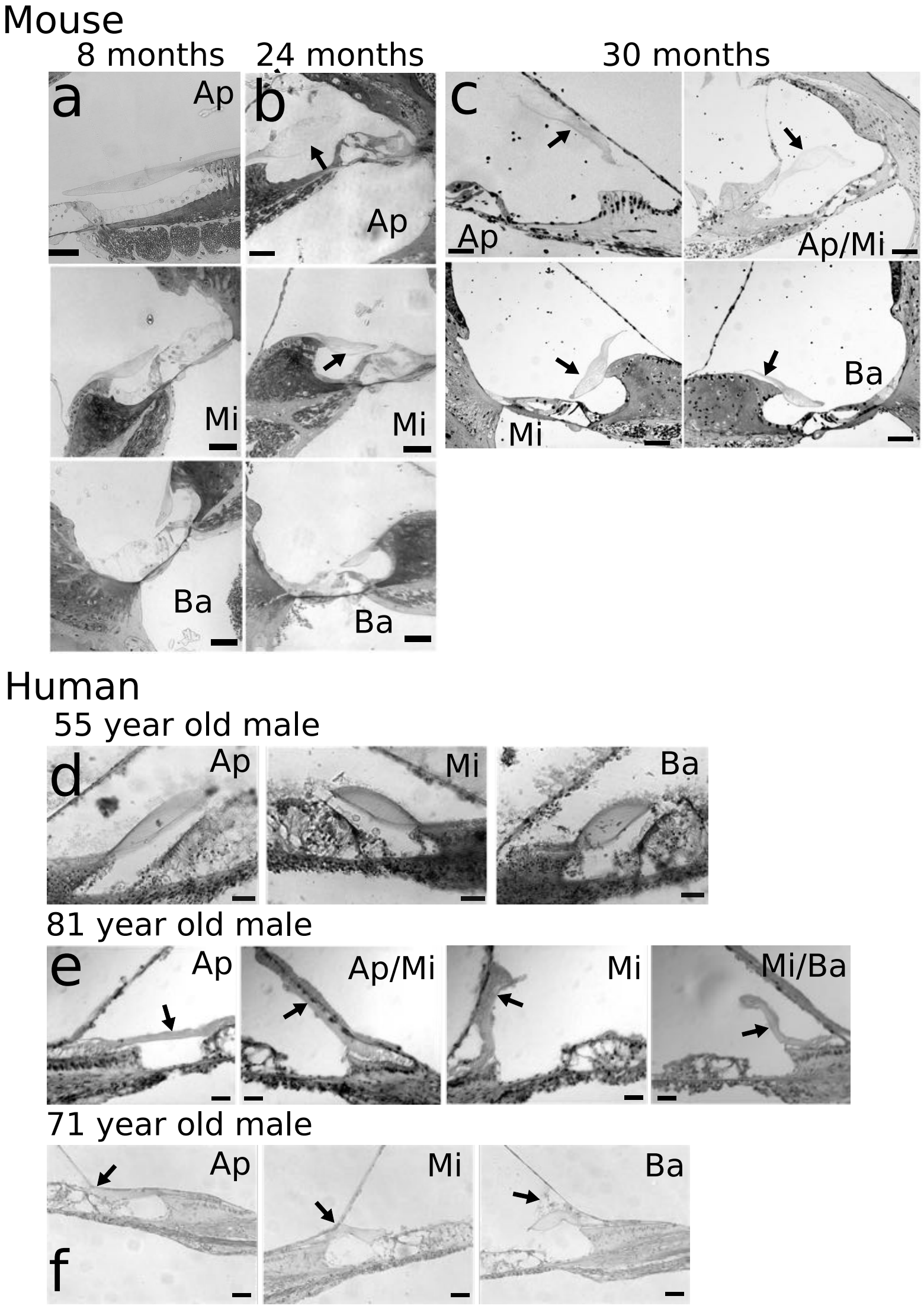
Mouse
8 months
24 months
30 months
a
Ap
b
Ap
c
Ap
Ap/Mi
Mi
Mi
Mi
Ba
Ba
Ba
Human
55 year old male
d
Ap
Mi
Ba
81 year old male
e
Ap
Ap/Mi
Mi
Mi/Ba
71 year old male
f
Ap
Mi
Ba

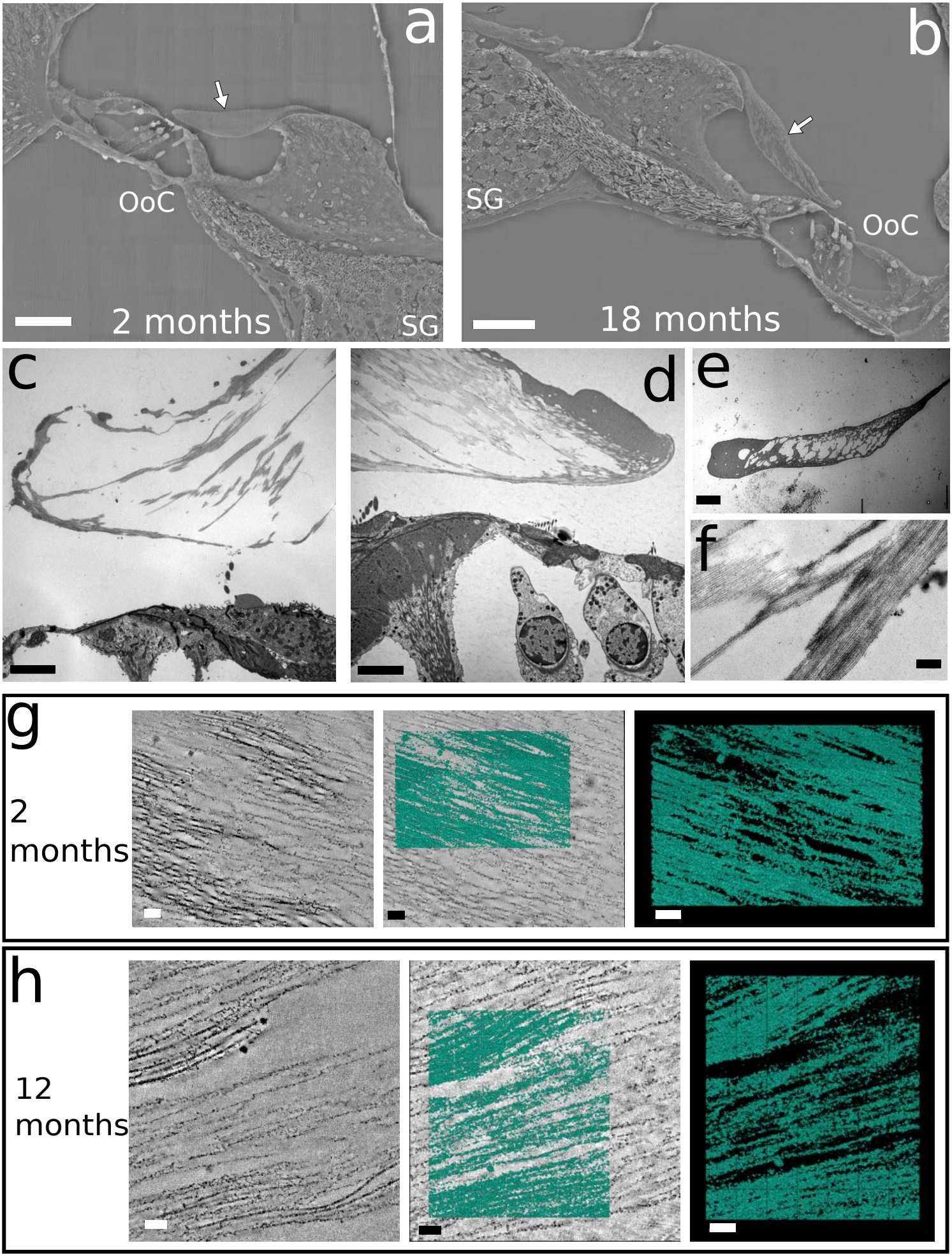
a
OoC
2 months
SG
b
SG
OoC
18 months
c
d
e
f
g
2
months
h
12
months

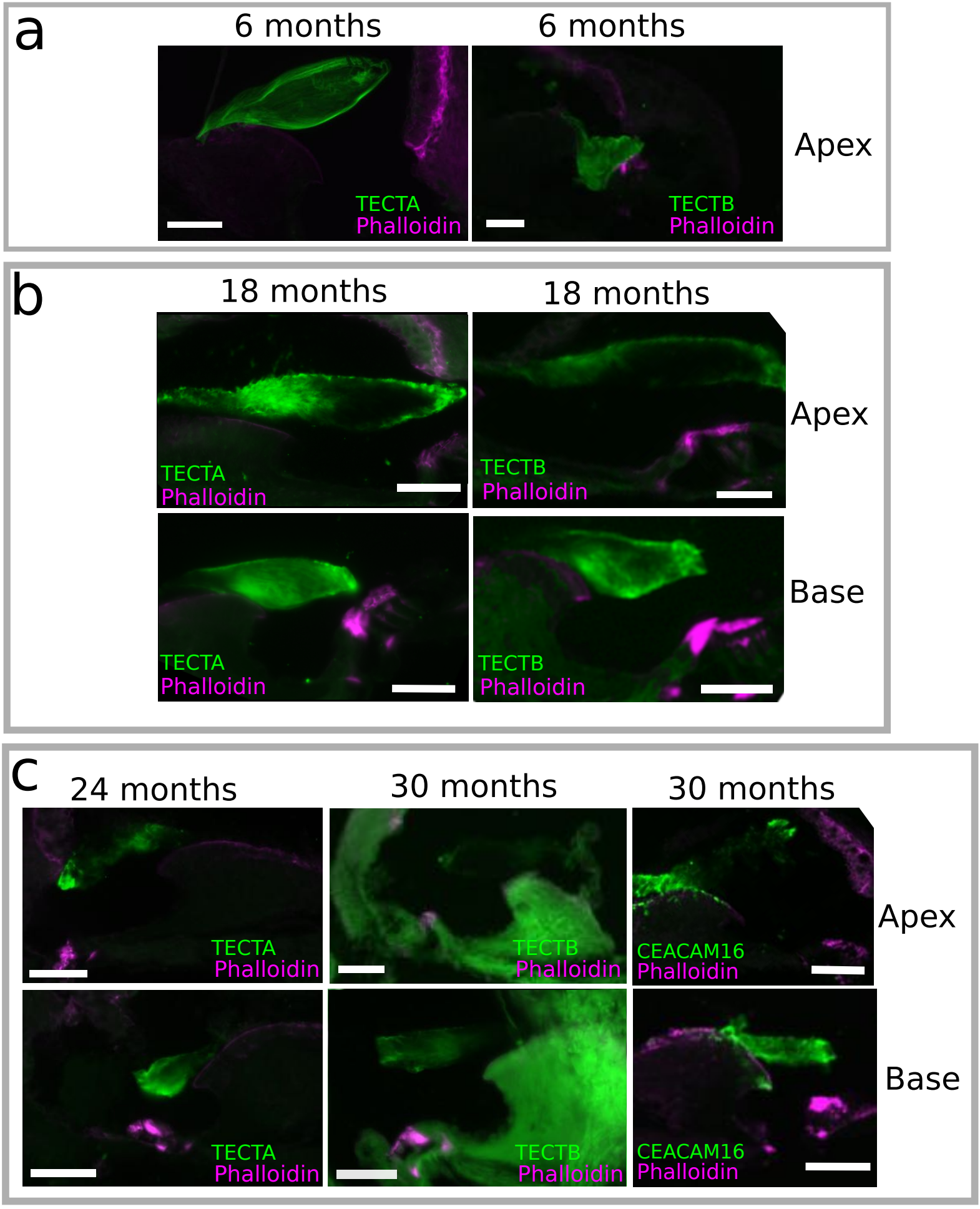
a
6 months
6 months
TECTA
Phalloidin
TECTB
Phalloidin
Apex
b
18 months
18 months
TECTA
Phalloidin
TECTB
Phalloidin
Apex
TECTA
Phalloidin
TECTB
Phalloidin
Base
c
24 months
30 months
30 months
TECTA
Phalloidin
TECTB
Phalloidin
CEACAM16
Phalloidin
Apex
TECTA
Phalloidin
TECTB
Phalloidin
CEACAM16
Phalloidin
Base